Astron. Astrophys. 283, 753–758 (1994)

ASTRONOMY
AND
ASTROPHYSICS

# CCD imaging of NGC 4861: morphology and brightness distribution

**H. Dottori**[1], **J. Cepa**[2], **J. Vilchez**[2], **and C.S. Barth**[1]

[1] Depto. de Astronomia, Instituto de Física – UFRGS, CP 15051, Porto Alegre, 91500, RS, Brasil
[2] Instituto de Astrofísica de Canarias, E–38200 La Laguna, Tenerife, Spain

Received 17 November 1992 / Accepted 3 August 1993

**Abstract.** We discuss narrow band CCD imaging of NGC 4861 in continua at 4500 Å, 5300 Å and 6300 Å as well as in H$\alpha$, H$\beta$ and [OIII] $\lambda$ 5007Å lines. We find that the system exhibits a double nucleus structure and a counter–tail to the well–known NE chain of HII regions. The mean value of lines and continua frames for the main body brightness distribution of NGC 4861 is $R^{-2.04\pm0.35}$, comparable to the Hubble–Reynolds law $R^{-2}$. The three mentioned characteristics indicate that NGC 4861 might have undergone a merger process. The time elapsed from the beginning of the phenomenon is set to be smaller than three crossing times. New observations are proposed to confirm or reject the merger scenario for this peculiar galaxy.

**Key words:** galaxies: individual: NGC 4861 – galaxies: interactions – galaxies: interstellar matter – galaxies: irregular

## 1. Introduction

Arp (1966) includes NGC 4861 (also known as I Zw 49, Arp 266, Mkn 59) in the class of galaxies with irregular knots. In his atlas, Arp describes the galaxy as being composed by bright knots scattered in a narrow N–S band, with a very bright knot (hereinafter BK) at the S–W extreme. In the Uppsala General Catalogue of Galaxies, NGC 4861 is classified as a bright knot of $0.35' \times 0.35'$, and magnitude $m_v = 13.2$, superimposed to the south end of IC 3961, with which it forms a double system. IC 3961 is an extended and diffuse blue galaxy, amorphous in appearance, of magnitude $m_v = 14.1$ without any trace of absorption. de Vaucouleurs et al. (1976) classify NGC 4861 (which is not distinguished from IC 3961) as SB(s)m (uncertain) with an angular size of 3.3 arcminutes and a systemic velocity of 831 Km/s. Kennicutt et al. (1989) carried out H$\alpha$ photographic photometry of this system, identifying 27 HII regions whose H$\alpha$ fluxes have been measured; they argue that the BK flux is 6 times larger than that of 30 Dor.

*Send offprint requests to*: J. Cepa

In what follows we adopt the UGCG identification, namely we differentiate the underlying irregular galaxy IC3961 (Fig. 1a) from NGC 4861. In Hodge's (1983) and our (Fig. 1b) H$\alpha$ image NGC 4861 appears composed by the BK and the emitting extentions.

The BK has been subject to extensive spectroscopical studies (Neugebauer et al. 1976; French & Miller 1983; Dinnerstein & Shields 1986). The two last papers derived a Helium abundance Y=0.216 and 0.23 respectively. The abundances of oxygen, nitrogen, neon and sulphur relative to hydrogen were reported to be similar to those of "isolated extragalactic HII regions" (IEHRs) (Sargent & Searle 1970) and well below what is considered to be solar. Dinnerstein & Schields 1986 found strong WR features, which also seem to be a common feature in the spectra of some IEHRs. The remarkable stellar make up of this type of objects, together with their very low content of heavy–elements, as deduced from the emission–line spectra, lead to the conclusion that they are either "young galaxies", forming their first generation of stars, or that at most they could have formed stars in short bursts separated by long quiescent phases (Sargent & Searle 1970; Baldwin et al. 1982).

We carried out CCD imaging of NGC 4861 in strong emission lines and nearby continua. This paper presents a morphological and brightness distribution study of the BK and its surrounding regions with the purpose of inferring the dynamical processes developing in this object. In Sect. 1 we present the observations, in Sect. 2 we discuss the morphology of NGC 4861, as derived from narrow band imaging; Sect. 3 is devoted to the analysis of the brightness distribution and Sect. 4 contains our conclusions and suggestions for future work on this galaxy.

## 2. Observations and reductions

We performed narrow band CCD imaging, with interference filters centred on the continua at $\lambda$4500 Å, 5350 Å and 6300 Å as well as lines H$\alpha$, H$\beta$ and [OIII] $\lambda$ 5007Å. The observations were carried out in a seven days run during February–March 1989 with the 1m Jacobus Kapteyn Telescope, in the Roque de los Muchachos Observatory, La Palma. In Table 1 we furnish the

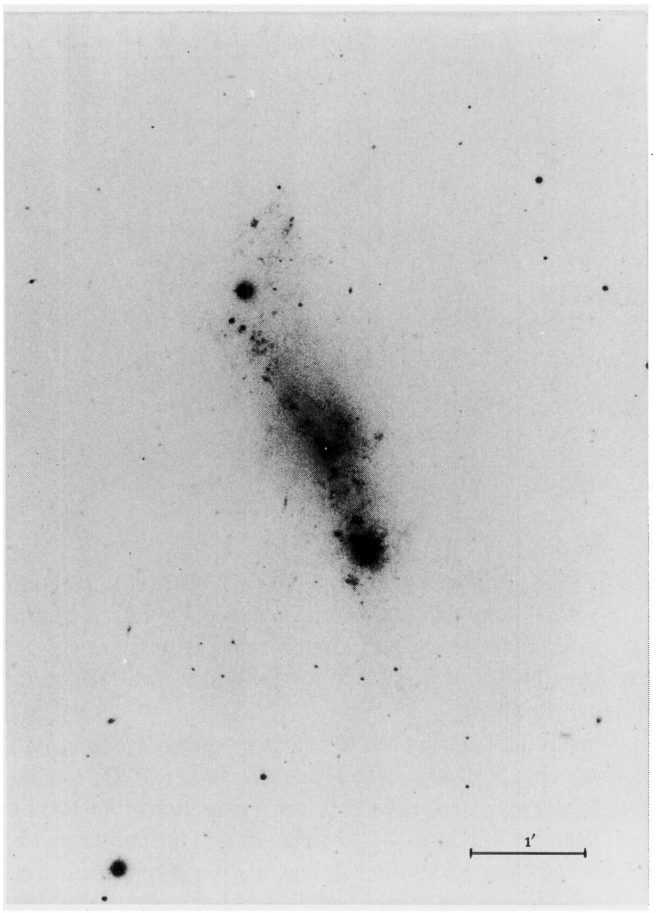


**Fig. 1a.** Image of NGC 4861 from Sandage & Bedke (1988). North is towards the top, East is towards the left. Scale as indicated

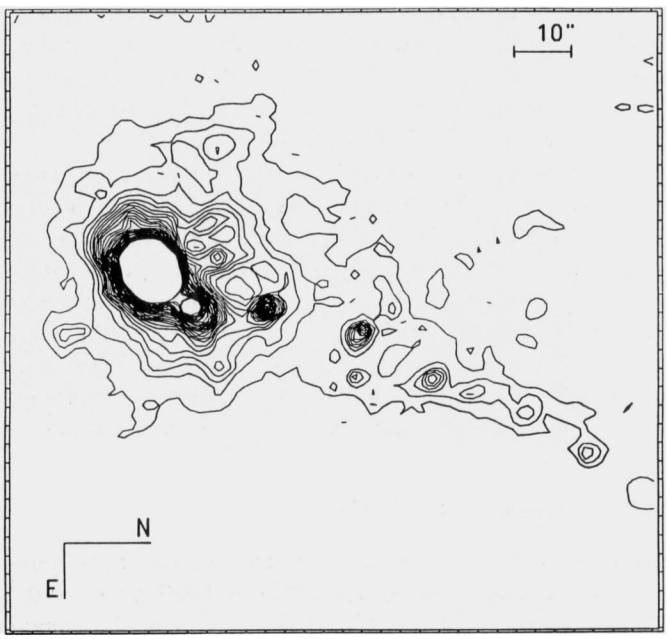


**Fig. 1b.** Hα image of NGC 4861. Scale and orientation as indicated

**Table 1.** Log of observations of NGC 4861 and the spectrophotometric standard HD 84937. The brackets in column 3 indicate the number of observations per filter. Exposure times are for each individual frame

| Date | Object | Filter | Exp. Time |
|---|---|---|---|
| 28 Feb | HD 84937 | Hα(2), Hβ(2), [OIII](2) | 20s |
| | | CHα(2), CHβ(2), C[OIII] | 6s |
| 2 Mar | HD 84937 | Hα(2), Hβ(2), [OIII](2) | 20s |
| | | CHα(2), CHβ(2) | 6s |
| | | C[OIII] (2) | 6s |
| 5 Mar | HD 84937 | Hα(2), Hβ(2), [OIII](2) | 20s |
| | | CHα(2), CHβ(2) | 6s |
| | | C[OIII] (2) | 6s |
| | NGC 4861 | Hα(2), CHα(3) | 1800s |
| | | Hβ(3), CHβ(1) | 1800s |
| 6 Mar | HD 84937 | Hα(2), Hβ(2), [OIII](2) | 20s |
| | | CHα(2), CHβ(2) | 6s |
| | | C[OIII] (2) | 6s |
| | NGC 4861 | Hα(3), CHα(2) | 1800s |
| | | Hβ(2), CHβ(3) | 1800s |
| | | [OIII](2), C[OIII] (3) | 1800s |

data yielded by the observations. 2.5 hours of integration were achieved in the Hα, Hβ and their respective continua, whereas 2.0 hours were reached in the [OIII] λ 5007Å and its continuum, under very good to good seeing conditions (0.8 to 1.2 arcsec).

Oke & Gunn's (1983) spectrophotometric standards have been observed, although an absolute calibration is not necessary for the present analysis. Data reduction and absolute calibration procedures were conducted using a SUN SPARCstation2 workstation, employing standard methods of the IRAF reduction package (for a complete description, the reader is referred to Barth et al. 1993).

The error is given by the Poissonian noise, because the distribution of brightness is analysed within each frame, without mixing images from different filters, except for the continuum subtraction. We obtained an error of less than 2% in the intensity for the continuum frames, and of about 3% in the line frames.

## 3. The morphology of the BK in NGC 4861

### *3.1. Low level isophotes*

Hodge's (1983) Hα photography of NGC 4861 reveals that the BK is a huge emission region, about 1.5 kpc ($H_o$ =100 km $sec^{-1}$ $kpc^{-1}$) in diameter, rich in morphological details, which is linked to a chain of HII regions extending northward (hereinafter *North tail*), in a projected line of more than 3 Kpc length, mildly curved to the East. In Fig. 2 we show the faintest isophotes at Hα , obtained by properly subtracting the continuum frame at 6300 Å from that centred at the Hα line. Due to the long exposure time added to these frames it was possible to detect a bow–like faint structure, connected to the BK. This faint structure (hereinafter *counter–tail*) extends roughly in the N–S direction, and is curved to the East, with a projected length of 1.9 kpc. Four HII regions are clearly detected on the counter–tail. One

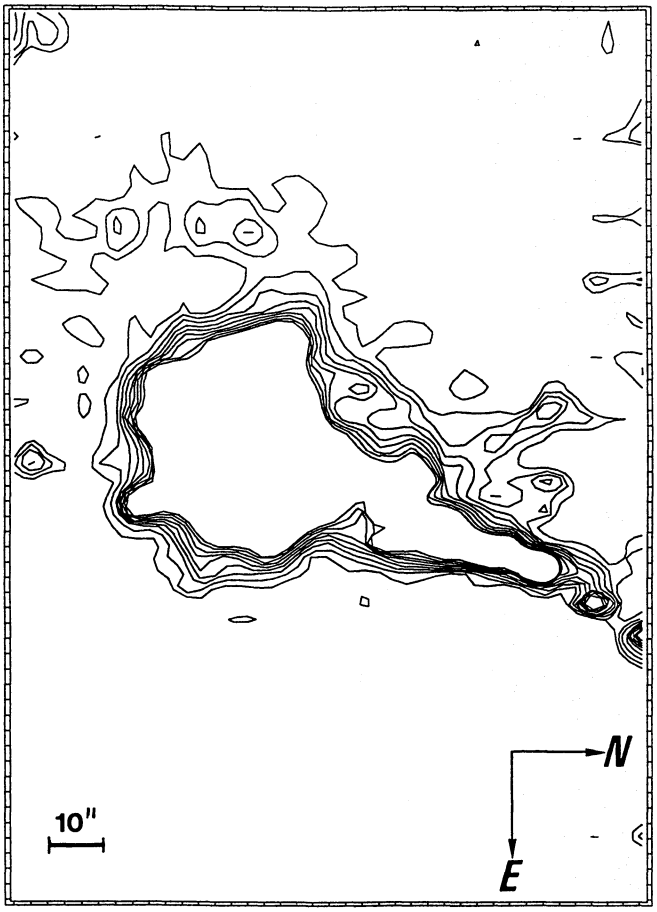


**Fig. 2.** Hα low level isophotal map. The counter–tail to the well–known North tail is clearly visible. Scale and orientation as indicated

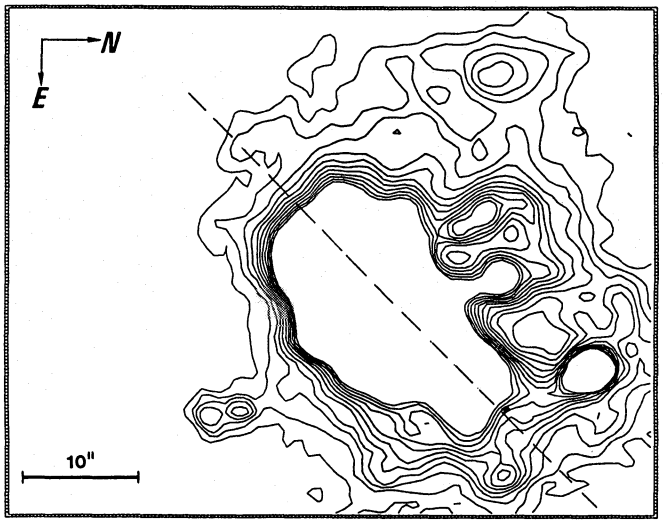


**Fig. 3.** Hα intermediate level isophotes. The wavy form of the internal isophotes reveals that they are modulated by the superposition of individual Strömgren spheres. The isophotes' major axis is North 47° East. Scale and orientation as indicated

of them, the HII region located at (X=142, Y=435, in Fig. 2) is also measurable in the continua and in the Hβ and [OIII] λ 5007Å lines. The counter–tail's total Hα flux is $10^{37}$ erg $s^{-1}$, or equivalently $2.1 \times 10^{49}$ Lyman photons per second, which needs about 5 O5 stars to be justified, or equivalently about 150 B0 stars. The extension, and mild brightness distribution of the counter–tail's Hα emission leads us to believe that it is mainly ionized by an extended distribution of B type stars with hotter stars contributing to the condensations.

### *3.2. The bright knot structure*

#### 3.2.1. Low level isophotes

The faintest Hα isophotes (Fig. 2), matching concentrically the BK symmetry, reach a diameter of about 2.8 Kpc, much larger than the 1 kpc measurement reported by French (1980), on the Palomar Sky Survey plates and larger than that obtained from the high contrast Hα photography contained in Hodge's Atlas of HII regions (1983). From Fig. 2 we obtain the true size of the *fuzzyball*, which is ionized by the leakage of Lyman photons from the star–forming regions conforming the BK, and which presumably trace the matter gravitationally linked to the BK. We discuss this point below.

The low–level brightness isodensities around the BK also exhibit plenty of outer loops, bridges and plumes, which strongly resemble the characteristics found in the IIZw40 (Baldwin et al., 1982) and in the larger merging system NGC7252, as described by Schweizer (1982).

#### 3.2.2. The intermediate level isophotes

At intermediate intensity levels, the BK's pure Hα frame presents rippled isophotes (Fig. 3). The wavy contours are due to the contact of different Strömgren spheres produced by the strong star formation taking place throughout the BK's main body, within the central 1.5 kpc. The diameter of these HII regions ranges from 200 to 350 pc. These starburst phenomena might have been triggered by a tidal mechanism, as transpires from Hernsquist's numerical simulations (1989). The present coeval cycles of star formation are together so intense in NGC 4861 that the whole ionized region centred in the BK extends from 2.5 to 3.0 kpc, as mentioned in the previous section, and furnishes the arguments by which this galaxy is generally included among the IEHRs (Neugebauer et al. 1976; French 1980; French & Miller 1983; Garnett 1989).

The BK's very low content of heavy elements and Helium (see the introduction) indicates that any star formation activity taking place in its interior, previous to the present one has been poor or even non existent from any practical point of view.

#### 3.2.3. High level isophotes

In Figs. 4a and 4b we show respectively the isodensity maps of the pure Hα line and the continuum at 6300 Å. A two condensations structure appears clearly in the Hα frame (Fig. 4a). Both blobs are separated by 110 to 130 pc (about 2 to 3 arcsec) and the NE nucleus is more intense than the SW one in

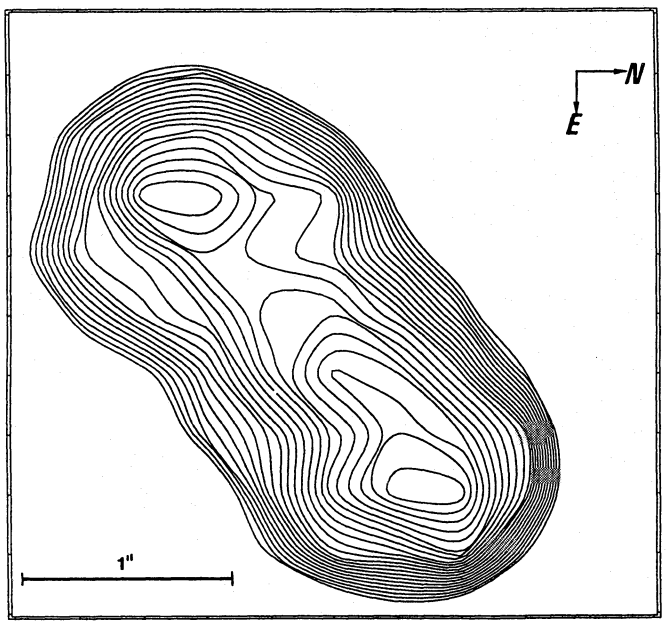


**Fig. 4a.** Hα internal isophotes showing the two nuclei structure. The line joining both condensations is North 50° East. The N–E condensation is more intense than the S–W one. Scale and orientation as indicated

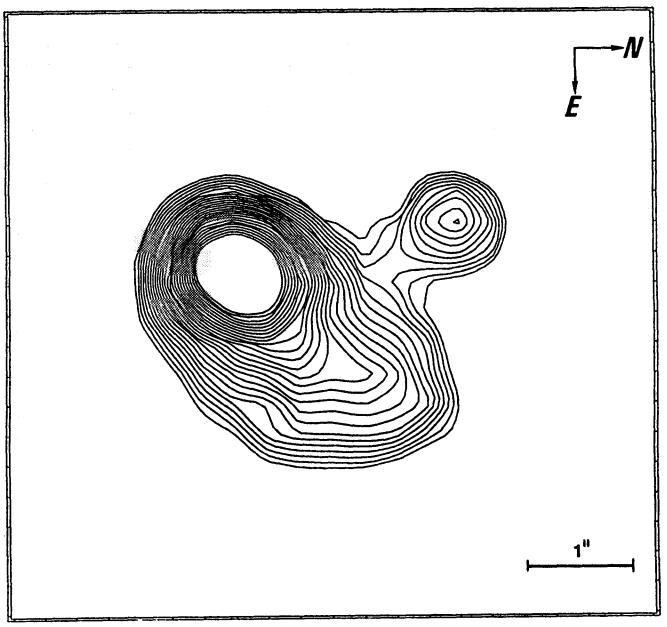


**Fig. 4b.** Internal isophotes for the continuum at 6300 Å. The strong S–W condensation coincides in position with the less intense blob in Fig. 3. It does not show a condensation coinciding with the Hα emitting N–W blob, but the ridge of the isophotes points in the same NW direction. A detailed discussion on the ionizing association is given in Section 2. Scale and orientation as indicated

this line. In the continuum light, the SW blob is more intense, the NE one being detected by a mild deformation introduced in the faintest isophotes (Fig. 4b). The different appearance of the condensations in line and continua frames can be interpreted as an evolutionary phenomenon. The NE blob might be at an earlier evolutionary phase, and hence may hold the most massive stars which provide the strong flux of ionizing photons necessary to explain its higher Hα luminosity. On the other hand, the SW one appears to be in a more advanced stage of evolution, with the more massive stars undergoing the RSG phase and some of them having reached the WC stage (for more details see Maeder's evolutionary tracks, 1990), which might explain the detection of WC features by Dinnerstein & Schields (1986). We are reporting for the first time the existence of a double condensation structure in the BK of NGC 4861. It is worth noting that if the object were located at twice the actual distance it would have been very difficult to detect the double condensation. This detection was also helped by the good seeing that prevailed during the observing run.

The region between both blobs presents isophotal deformation, in line as well as continuum maps, indicating the influence of an interaction disturbing the brightness distribution. The isophotes embracing both condensations do not present either deformations or signatures of rotation, the major axis being aligned with that of the intermediate level isophotes, with an orientation N 48° E.

The size of the features in between and around both condensations more or less match the resolution of the observing system plus seeing, so one must be cautious when deriving more substantial conclusions on the basis of these morphological aspects.

## 4. The BK brightness distribution

This section analyses the BK brightness distribution in the Hα, Hβ, and [OIII] λ 5007Å frames, as well as in the continua at 4500 Å, 5300 Å and 6300 Å frames.

We assigned each isophote of intensity **I** an *equivalent radius* **R** (de Vaucouleurs et al. 1976). In Figs. 5 and 6 we present the behaviour of log I vs log R, for the continuum at 6300 Å and the Hα emission line, representative of continua and line density profiles, respectively. Figures 5 and 6 also show the linear regression and its reddening corrected value. The internal reddening was derived from the ratio Hα/Hβ, averaged in concentric rings centred at the BK. For comparison we plotted the $R^{-1}$, $R^{-2}$ and $R^{-3}$ and de Vaucouleurs' surface brightness distribution laws. We see that the slope of the three continua are slightly shallower than the $R^{-2}$, while the slopes of the three emission lines is slightly steeper.

The linear regression for the brightness distribution in the Hα, Hβ and [OIII] λ 5007Å is −2.30, −2.09 and −2.53 respectively while for the continua at 4500 Å, 5300 Å and 6300 Å is −1.62, −1.67 and −1.61 respectively.

The reddening corrected mean slope obtained from the 6 different regressions is $-2.04 \pm 0.35$, surprisingly similar to the projected brightness distribution $R^{-2}$ or Hubble–Reynolds law, and also to the $R^{1/4}$ de Vaucouleurs law. The observations cover

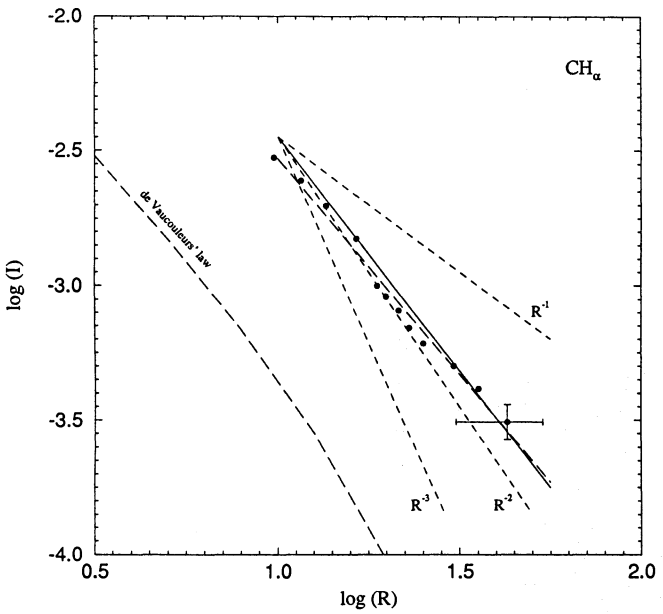


**Fig. 5.** The Bright Knot (BK) surface brightness distribution (empty dots) in the H$\alpha$ continuum. The de Vaucouleurs, Hubble–Reynolds (R$^{-2}$), R$^{-3}$ and R$^{-1}$ laws of surface brightness distribution are shown for comparison. The long dashed lines represent the best fit to the measurements, and the full line is the reddening corrected regression. Error bars are calculated from poissonian statistics

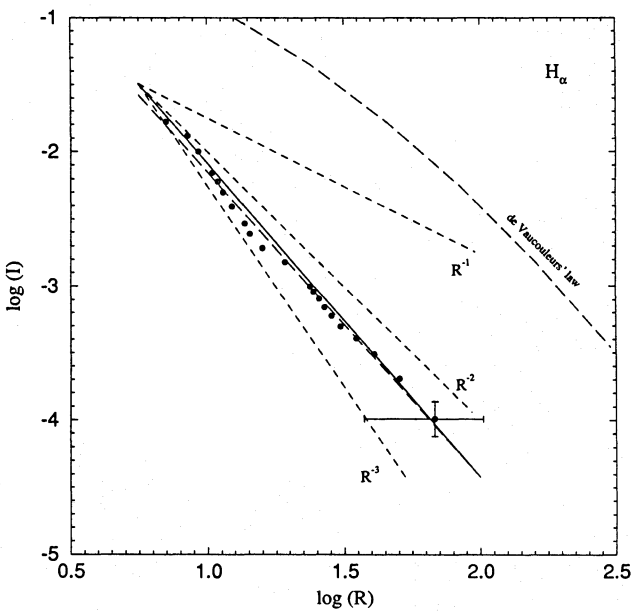


**Fig. 6.** The Bright knot (BK) brightness distribution in the H$\alpha$ line. Remarks as in Fig. 5

more than 1 and 2 decades in log I for the lines and continua respectively.

## 5. Possible scenarios

Two possible scenarios related to tidal interactions might give clues to explain the morphological characteristics of NGC 4861.

1) The first possibility is the tidal disruption of the main body of NGC 4861 by IC 3961, which might explain the double nucleus structure. The *North tail* of the HII region could be an external arm of IC 3961, extending inwards not too deeply in the IC 3961 disk, which would explain the lack of absorption in these HII regions, as derived from the H$\alpha$/H$\beta$ ratio. NGC 4861 could be an external giant HII region similar to NGC 604 in M 101, or 30 Dor in the LMC.

If we consider the expression for the tidal radius (Lang 1980),

$$\frac{M_G}{M_{BK}} = 0.33 \left(\frac{d}{r_t}\right)^3$$

where $M_G$ is the IC3961 mass, $M_{BK}$ that of the BK, $d$ is the distance between the center of IC 3961 and that of the BK and $r_t$ the distance between the BK central condensations, we can obtain a rough estimate of IC 3961 mass. If the star formation within the BK follows an IMF with $1.45 \leq x \leq 2.0$, the H$\alpha$ luminosity of the BK ($L_{BK} = 2 \times 10^{40} erg\ s^{-1}$) would lead to a total mass $2.2 \times 10^6 \leq M_{BK}/M_\odot \leq 7 \times 10^6$. If the real $d$ and $r_t$ are of order the projected ones, $d \sim 65$ arcsec and $r_t \sim 2$ arcsec, we obtain for IC 3961 $2 \times 10^{10} \leq M_G \leq 7 \times 10^{10}$, which is of the same order as the LMC mass, IC 3961 being somewhat smaller in size. The smooth brightness distribution of the BK conspires against this scenario, because it is difficult to imagine that a tidal force, influencing the object so deeply, would not be affecting its outermost matter distribution.

2) In a second scenario, also in terms of tidal forces, The BK might be undergoing a merge. Much work has been devoted to date to understand the collision of galaxies from a theoretical point of view (White 1979; Farouki & Shapiro 1982; Negroponte & White 1983; Barnes 1988; Borne & Richstone 1991; etc), as well as to conduct a detailed study of individual systems, which are either clear cases of collision or present one or more characteristics connected to this type of phenomenon (see Schweizer 1982; Fried & Schulz 1983; Colina et al. 1991; Mirabel et al. 1991; Balcells & Stanford 1990).

As shown in Section 3, the BK brightness distribution follows the Hubble–Reynolds law, as predicted by White (1979) for advanced stages of the merging process. Collisions of large galaxies such as NGC 7252 (Schweizer 1982) already show this brightness distribution.

Regarding starbursts triggered by merger processes in IGHR, the class of objects to which NGC 4861 belongs, Baldwin et al. (1982) also argued in favour of a collision of two extremely small galaxies to explain the present burst of star formation in II Zw 40. This object presents, moreover, a double tail protruding from a halo, which is composed of small optically thick filaments.

The separation between both blobs in the BK is about 5% of the roughly spherical distribution of matter around the BK center. White's (1979) numerical simulations (see also Negroponte & White 1983; Farouki & Shapiro 1982) lead to an elapsed

time smaller than three crossing times since the beginning of the merger for this type of configuration. From the point of view of merger evolution it is in a less advanced stage of evolution than NGC 7252.

If the tail and counter–tail of Fig. 2 are byproducts of an ongoing merging process within the BK, then a remnant of net internal angular momentum is to be expected, at least within one of the two condensations. In fact the models (White, 1979, Borne & Richstone, 1991) predict that one or both colliding objects must have internal rotation in order to form antennae like features. As Balcells & stanford (1990) pointed out for Arp 155 (NGC 3656) this object presents an ortho–rotating double core, and provides strong evidence linking kinematically peculiar cores to mergers. Spectroscopy of the BK innermost structure will help to further check the merger scenario for NGC 4861.

## 6. Discussion and conclusions

We have carried out narrow band CCD imaging of NGC 4861 at the continua at 4500 Å, 5300 Å and 6300 Å as well as at the lines H$\alpha$, [OIII] $\lambda$ 5007Å and H$\beta$. Long integration times and very good seeing conditions ensured outstanding richness of details in our composed frames.

We report for the first time the existence of a double core as well as the detection of a faint structure that extends southward from the main body (BK) of NGC 4861, which we interpret as a counter–tail to the already known North tail. Both types of structures, the double core and the two tails, are tracers of merging processes, and are detected in many Antennae like systems. Their coeval existence indicates that the merging process is not older than 3 crossing times.

The continua's two–dimensional brightness distribution is slightly shallower than the $R^{-2}$ Hubble–Reynolds law, whereas that of the emitting gas is slightly steeper.

The very low metallicity of this object would indicate that the present one is the first important starburst experimented by NGC 4861. Collision–triggered starbursts are not strange events among IEHRs (Brinks & Klein, 1988).

According to these arguments we suggest that NGC 4861 is currently undergoing a merger, which is not in an extremely advanced stage of evolution. Taking into account the small size of the whole system we suggest it is characterized as a *Mini–antennae*.

We have embarked on a project to perform long slit spectroscopy of the tails, in order to check their relative movement, and that of the BK, in a similar fashion as Balcells & Stanford (1990) for NGC 3656, and also to determine the relative movement of the two nuclei. Specific numerical experiments, like those developed for NGC 7252, could very much help to understand the kinematics of this interesting galaxy. The morphological and kinematical study of IC 3961 will assist us in understanding its connection to NGC 4861.

*Acknowledgements.* The Jacobus Kapteyn Telescope is operated on the island of La Palma by the Royal Greenwich Observatory in the Spanish Observatorio del Roque de Los Muchachos of the Instituto de Astrofísica de Canarias. This work was partially supported by the Brazilian institutions CAPES and CNPq. JC and JV acknowledge partial support through grants no. PB89–0510 and PB91–0525 from the DGICYT (*Dirección General de Investigación Científica y Técnica*) of the Spanish *Ministerio de Educación y Ciencia.*

## References

Arp, A. 1966, ApJS, 14, 1
Balcells, M., Stanford, S.A. 1990, ApJ, 362, 443
Baldwin, J.A., Spinrad, H., Terlevich, R. 1982, MNRAS, 198, 535
Barnes, J.E. 1988, ApJ, 331, 699
Barth, C., Cepa, J., Vilchez, J., Dottori, H. 1993, AJ, submitted
Borne, K.D., Richstone, D.O. 1991, ApJ, 369, 111
Brinks, E., Klein, U. 1988, MNRAS, 231, 63p
Colina, L., Sparks, W.B., Macchetto, F. 1991, ApJ, 370, 102
Dinerstein, H.L., Shields, G.A. 1986, ApJ, 311, 45
Farouki, R.T., Shapiro, S.L. 1982, ApJ, 259, 103
French, H.B. 1980, ApJ, 240, 41
French, H.B., Miller, J.S. 1983, ApJ, 248, 468
Fried, J.W., Schulz, H. 1983, A&A, 118, 166
Garnett, D.R. 1989, ApJ, 345, 282
Hernquist, L. 1989, Nat, 340, 687
Hodge, P. 1983, AJ, 88, 296
Kennicutt, R.C. jr, Edgar, B.K., Hodge, P.W. 1989, ApJ, 337, 761
Lang, K.R. 1980, Astrophysical Formulae, Springer–Verlag
Maeder, A. 1990, A&AS, 84, 139
Mirabel, I.F., Lutz, D., Maza, J. 1991, A&A, 243, 367
Negroponte, J., White, S. 1983, MNRAS, 205, 1009
Neugebauer, G., Becklin, E.E., Oke, J.B., Searle, L. 1976, ApJ, 205, 29
Oke, J.B., Gunn, J.E. 1983, ApJ, 266, 713
Sandage, A., Bedke, J. 1988, Atlas of galaxies useful for measuring the cosmological distance scale, NASA SP;496
Sargent,W.L.W., Searle, L. 1970, ApJ, 162, L155
Schweizer. F. 1982, ApJ, 252, 455
White, S. 1979, MNRAS, 189, 831
Vaucouleurs, G. de, Vaucouleurs, A. de, Corwin, H.G. 1976, Second Reference Catalogue of Bright Galaxies. University of Texas Press, Austin

This article was processed by the author using Springer-Verlag LaTeX A&A style file version 3.